

The nature of ‘overexchanged’ copper and platinum on zeolites

Marc Schreier¹, Sarah Teren¹, Latonia Belcher¹,
John R Regalbuto^{1,3} and Jeffrey T Miller²

¹ Department of Chemical Engineering, University of Illinois at Chicago, 810 S Clinton, Chicago, IL 60607, USA

² BP Research Center, 1510 W Warrenville Road, Naperville, IL 60563, USA

E-mail: jrr@uic.edu

Received 31 March 2005, in final form 6 May 2005

Published 7 June 2005

Online at stacks.iop.org/Nano/16/S582

Abstract

The uptake of platinum and copper tetra-ammine (PTA and CTA, $[(\text{NH}_3)_4\text{Pt}]^{2+}$ and $[(\text{NH}_3)_4\text{Cu}]^{2+}$) into zeolites was compared over silica and three zeolites (Y, MOR and MFI) with different points of zero charge and aluminium content. Adsorption was determined as a function of pH at several metal concentrations, and pH shifts relative to metal free control experiments were carefully monitored.

The uptake of both metal ammine complexes onto silica is well described by electrostatic adsorption. We suggest that the metal cations interact with zeolites by two mechanisms, ion exchange at the Al exchange sites and electrostatic adsorption at silanol groups. The former is the dominant mechanism at low to mid pH, and the latter at high pH. This effect is most clearly manifested in zeolites with low aluminium content such as ZSM5; electrostatic adsorption at high pH in ZSM5 yields metal loadings much in excess of the ion exchange capacity and so gives rise to ‘overexchange’.

Differences between PTA and CTA can be explained by the weaker stability of the CTA complex and its response to the decrease in local pH near the adsorption plane of low PZC zeolites. This change in local pH near oxide surfaces is characteristic of electrostatic adsorption. As the local pH decreases, the CTA ion is probably converted to a dimerized copper complex, perhaps $\text{Cu}_2(\text{OH})_2^{2+}$. A portion of the released ammonia is protonated, increasing the solution pH. In high PZC, high aluminium zeolites with high ion exchange capacity, there is relatively little contribution from electrostatic adsorption.

1. Introduction

Nearly two decades ago, Iwamoto and co-workers [1, 2] discovered that ‘over’- or ‘excessively’ exchanged copper on the MFI (ZSM5) zeolite was a highly active catalyst for the lean NO_x reduction to N_2 . In these catalysts, the amount of copper(2+) ion exceeded the 1:2 ratio assumed by the ion exchange reaction



³ Author to whom any correspondence should be addressed.

They developed two methods to make Cu/ZSM5 catalysts. The first employed repeated ion exchange of the ZSM5 with solutions of copper acetate [1]. Three to four ion exchanges were required to obtain high metal loading. Similar methods were subsequently developed by altering the solution contact time (from 24 to 72 h) and solution temperature [3–6], and in some cases where extremely high weight loadings were desired adding Cu salts by dry impregnation [6].

Iwamoto and co-workers also prepared active catalysts by a single-step ion exchange of Cu(II) in basic ammonia hydroxide (NH_4OH). These ‘overexchanged’ Cu/ZSM5 catalysts were more active and selective than the previous

catalysts [2]. Iwamoto proposed that by raising the pH of the solution copper hydrolysis products form and the exchange species was $[\text{CuOH}]^+$, allowing 1:1 exchange with aluminium sites [7–9]. Other studies have suggested other exchangeable species, including $[\text{Cu}_2\text{OH}]^{3+}$, $[\text{Cu}_2(\text{OH})_2]^{2+}$ and $[\text{Cu}_3(\text{OH})_2]^{4+}$, in which the valence of copper remains 2+, but the charge per copper ion is less than 2 [9]. Following metal addition, copper is present as Cu(II) [10–14]. Using a variety of spectroscopic and analytical methods (EPR, EXAFS, XANES etc), Sachtler and co-workers [13, 14] and others [4, 9, 11, 12] believe that a copper dimer is exchanged, possibly the $[\text{Cu}_2(\text{OH})_2]^{2+}$ species. Iwamoto and Sachtler propose that a copper dimer is also the catalytic site for deNO_x reduction, although reduction of the dimer in overexchanged catalysts was found to yield a mixture of Cu(II), Cu(I) and Cu^0 at the surface [8–16].

Recently, we have demonstrated that 'strong electrostatic adsorption' (SEA) occurs at high pH between PTA cations and negatively charged, deprotonated hydroxyls on the silica surface [17]. Several studies suggest that an electrostatic adsorption mechanism may also apply under certain conditions on some zeolites. Chester and co-workers reported that highly silicious zeolites exhibit intracrystalline ion exchange of PTA under basic conditions in excess of the framework alumina content [18]. They associated this excess exchange capacity with the presence of internal silanol groups [19]. These studies concluded that there were two distinct adsorbed platinum species: one at the aluminium exchange sites and the other exchanged at silanols. Smirnov and co-workers similarly used PTA hydroxide to obtain 'overexchanged' platinum ZSM5 catalysts [20].

Copper forms the tetra-ammine $[\text{Cu}(\text{NH}_3)_4]^{2+}$ cation (CTA) above a pH of 9 with the addition of NH_4OH [21–26]. The stability of CTA improves in ammonium nitrate electrolyte solutions [21]. Louis and co-workers showed that CTA readily adsorbs onto silica in basic pH [21–23]. Arrua and co-workers also adsorbed CTA onto silica [24, 25]. In addition, in mordenite deNO_x catalysts the uptake of copper increased in ammonia [27–33]. However, none of these studies attempted to identify the adsorbing Cu species.

We hypothesize that the interaction of metal ammine cations with zeolites involves both ion exchange and electrostatic adsorption mechanisms; the latter is pH dependent, occurs on silanol groups, and is responsible for the 'overexchanged' metal loading.

The interplay between these two mechanisms is illustrated in figure 1. In figure 1(a) three separate uptake curves are represented. The first is for pH-independent ion exchange (IE) of the metal complex at Bronsted acid sites, which for a zeolite with an alumina content of 1 wt% and a surface area of $450 \text{ m}^2 \text{ gm}^{-1}$ (typical of H-ZSM5) yields a metal surface density of $0.4 \mu\text{mol m}^{-2}$. The second curve is for pH dependent 'strong electrostatic adsorption' (SEA) of cations at the deprotonated and so negatively charged surface hydroxyl groups. This curve has a characteristic volcano shape due to low surface charge at pH values close to the PZC, and low adsorption equilibrium constants at the high ionic strength pH extreme [17, 31–34]. The narrow pH range of SEA exists where surface charge is strong and ionic strength is low. If both mechanisms are operative, the hybrid third curve would

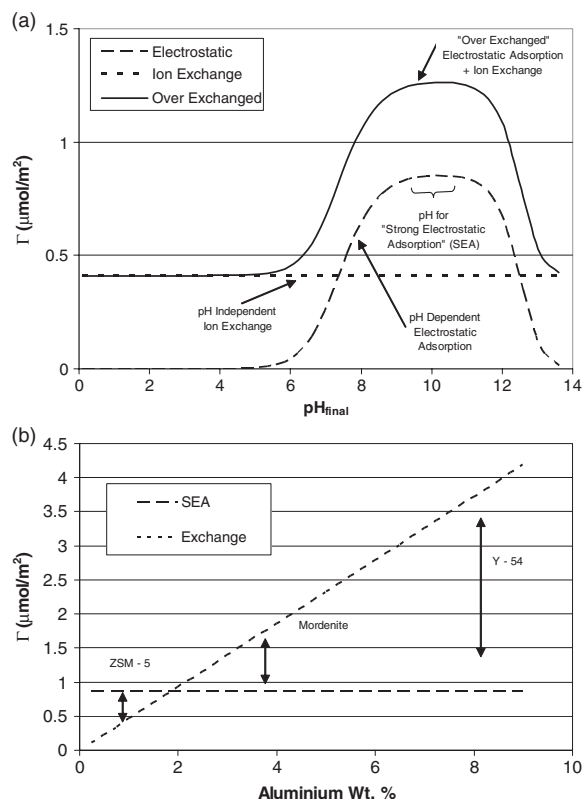


Figure 1. Hypothesis for 'overexchanged' zeolites: (a) ion exchange and electrostatic adsorption as a function of pH, (b) maximum SEA (dashed line) and IE (dotted line) surface density ($\mu\text{mol m}^{-2}$) versus aluminium weight per cent in zeolites.

be produced, in which ion exchange is augmented by SEA. Thus overexchange is postulated to occur only at high pH and to be electrostatic in nature.

The relative importance of SEA versus IE is dependent on the aluminium content and surface area of the zeolite. This is illustrated in figure 1(b), in which the maximum surface density of exchanged and electrostatically adsorbed Pt is plotted versus wt% Al in a zeolite of surface area $400 \text{ m}^2 \text{ gm}^{-1}$. Our previous work has revealed the maximum uptake of PTA over silica to be about one complex per 2 nm^2 , and corresponds to a close packed layer of complexes that retain two hydration sheaths [17, 35]. The corresponding surface density, $0.86 \mu\text{mol m}^{-2}$, is shown as the dashed line in figure 1(b). The maximum amount of platinum able to exchange into zeolites is determined by the aluminium content; the dotted line in figure 1 represents 100% exchange of metal and increases linearly with Al content. Two regimes are delineated; to the left of the intersection of the SEA and exchange curves, maximum uptake by SEA can be much greater than by IE. Such would be the case for typical ZSM5 materials, which contain relatively little aluminium. The ZSM5 and ZSM11 materials employed by Chester *et al* [18, 19] were in this range. The ZSM5 used in this study contained 1.0% Al by mass and is indicated on the figure. On the other hand, to the right of the intersection ion exchange is greater than the SEA maximum and overexchange becomes negligible at high Al contents. We have employed two zeolites in this

Table 1. Support parameters and experiment conditions.

Supports	Supplier	Surface area (m ² g ⁻¹)	Pore opening (Å)	Al (wt%)	PZC	Platinum adsorption			Copper adsorption		
						Grams support	Surface loading (m ² l ⁻¹)	Conc (ppm)	Grams support	Surface loading (m ² l ⁻¹)	Conc (ppm)
Silica (Vn-3s)	Degussa	175	—	—	4.0	0.571	2000	60	0.571	2000	60
								350			350
								60			60
H-ZSM5	Zeolyst	450	5.5 × 5.1	1.0	3.0	0.222	2000	—	0.222	2000	160
								350			350
								60			60
Na mordenite	UOP	398	7.0 × 6.5	3.87	6.0	0.057	453	160	0.171	1361	160
								400			350
								60			60
Na-Y54	UOP	641	7.4	8.91	10.0	0.025	319	160	0.075	957	160
								400			350
								400			350

regime, one with 3.9 wt% Al (Na-MOR) and another with 8.9% (Na-Y54).

In this paper, the uptake of PTA and CTA over a wide range of pH and metal concentrations was determined on silica and three zeolites (Y, MOR and MFI). We conclude that strong electrostatic adsorption occurs in low Al zeolites at high pH and gives rise to an overexchanged capacity. In high Al zeolites, however, the ion exchange capacity is high and minimal electrostatic adsorption is observed.

2. Experimental details

The properties of the silica and the Y, MOR and MFI zeolites are given in table 1. The minimum pore openings of each zeolite should be sufficient to accommodate the PTA complex, which has a radius of 4.82 Å. The point of zero charge (PZC) of the silica and zeolites was determined by the measurement of equilibrium pH at high oxide loading (EpHL) [36]. An important property of preparation studies is the surface area per volume of solution (m² l⁻¹), or the surface loading:

Surface loading (m² l⁻¹)

$$= \left(\frac{\text{Specific area (m}^2 \text{ g}^{-1}) \cdot \text{Mass (g)}}{\text{Volume of solution (l)}} \right).$$

The surface loading of silica and MFI was 2000 m² l⁻¹ with Pt concentrations (60 and 350 ppm) corresponding to 20 and 100% of electrostatic monolayer coverage based on a surface density of 0.86 mmol m⁻² for PTA [17, 35], or 50 and 250% of ion exchange based on the Al content of ZSM5. The surface loadings for Y and MOR were varied to correspond to 50, 100 and 250% of ion exchange capacity. The surface loadings employed with CTA were approximately three times higher those for PTA due to the difference in molecular weight of Pt and Cu.

Prior to measuring the PTA and CTA uptakes, a control experiment was performed in the absence of metal ions in order to determine the shifts in pH due to protonation or deprotonation of the surface hydroxyl groups. These can lead to large changes in the solution pH and have previously been described for silica [17].

The details for strong electrostatic adsorption (SEA) of PTA on silica have been given previously [17]. The PTA (from

Aldrich) solutions at various concentrations were adjusted to different initial pH values by the addition of HCl or NaOH. 50 ml of PTA solution was contacted with the zeolite and shaken for an hour and then approximately 5 ml of solution was filtered. The PTA remaining in solutions was determined by ICP. The final pH was also measured at this time. A number of measurements made at 24 and 48 h confirmed that equilibrium was achieved in the one hour contact time.

A similar procedure was used for adsorption of CTA, which was prepared using Cu(NO₃)₂·2.5H₂O (Aldrich) and NH₄OH. Copper nitrate was dissolved in deionized water to obtain a 10 000 ppm stock solution, which was confirmed with ICP analysis. A measured volume of stock solution was added to a 250 ml volumetric flask in order to obtain 60, 160 and 350 ppm copper. Deionized water and nitric acid were added to obtain solutions at pH values below 6.0. The dilute solutions were light blue in colour. Concentrated NH₄OH was added to the volumetric flasks containing dilute copper nitrate in order to obtain CTA solutions at pH values above 9. For pH values above 12, NaOH was added. The CTA solutions were dark blue. ICP analysis of the solutions was used to determine if any precipitation occurred. At pH values between 6 and 9 it was not possible to prepare Cu solutions due to significant precipitation. The pH adjusted solutions were added to the silica and zeolites. The mixtures were shaken for 1 h, 5 ml of solution was filtered for ICP analysis and final pH values were measured.

3. Theory—the revised physical adsorption (RPA) model

The RPA model used to simulate the data has been published previously [17, 31–33]. The model employs a Langmuir isotherm in which the adsorption constant is calculated from the Coulombic interaction between the charged complex (PTA and CTA) and the potential at the plane of adsorption.

The maximum extent of adsorption, Γ_{max} , for the cationic Pt ammine complex has been experimentally determined [17] to be a close packed layer of Pt complexes which retain two hydration sheaths. Based on the radius of PTA of 2.41 Å, and two diameters of water 2.76 Å, this maximum density is calculated to be 0.86 μmol m⁻², or about one complex

per 2 nm^2 . The other model parameters are the PZC, the OH density N_S , and the hydroxyl protonation/deprotonation constants expressed at $\text{p}K_1 - \text{p}K_2 = \Delta\text{p}K$. The PZC and $\Delta\text{p}K$ values are determined independently of adsorption, as detailed in [17], while the literature value of 5 OH nm^{-2} is used for silica and all zeolites. Model results are very insensitive to N_S , which mitigates the need for a precise value for the zeolites.

4. Results

The pH of aqueous solutions is strongly affected by the addition of catalyst supports like silica [17, 31–33, 36]. For example in figure 2(a), for an aqueous solution at an initial pH of 9, addition of silica leads to a decrease in pH to about 5. These shifts are due to the acid–base hydrolysis equilibrium of water by the support hydroxyl groups [36]. The solid line represents a pH model of silica based on the point of zero charge and the two equilibrium constants. The model slightly over estimates the pH above about 10. Figure 2(a) also shows the effect on pH for 60 and 350 ppm solutions of PTA and CTA. The pH shift for PTA is identical to that of water, which indicates that proton transfer does not accompany PTA adsorption as previously suggested [17]. For adsorption of CTA, however, there is a significant increase in the pH between a pH of 9 and 12. The pH shift is identical for the two CTA concentrations.

The PTA uptake at the two concentrations is shown in figure 2(b). The dashed curve is a prediction of the RPA model for silica using the parameters previously determined [17]. At low pH PTA ions are not adsorbed, while at pH values above about 7 there is significant adsorption of PTA. At the lower concentration there is insufficient PTA to give monolayer coverage and virtually all the Pt is adsorbed. At the higher PTA concentration the adsorption capacity increases until a pH of about 10. At this pH, surface coverage approaches an electrostatic monolayer as almost all the Pt is adsorbed. At pH values above 12 the adsorption capacity decreases due to the increased ionic strength of the solution [17, 31–33]. The RPA model fits the adsorption Pt reasonably well over the entire pH range.

The uptake of Cu ions on silica is shown in figure 2(c). As with PTA, copper(2+) ions, i.e., $\text{Cu}(\text{H}_2\text{O})_6^{2+}$, do not adsorb on silica at low pH. The pH range between 6 and 9 was avoided since copper hydrolysis products precipitate at these pH values. Above pH 9 the Cu ammine is stable. Between a pH of 9 to 10, the adsorption capacity of CTA is similar to that of PTA. Unlike PTA, however, further increases in pH lead to further adsorption of CTA. Maximum uptake is about $1.8 \mu\text{mol m}^{-2}$ or more than double that observed for PTA on silica. This corresponds to about two-thirds of the 350 ppm Cu initially in solution.

Adsorption results over H-ZSM5 are shown in figure 3: the pH shifts and uptake of PTA in figures 3(a) and (b), and the corresponding data for CTA in figures 3(c) and (d). Much of the Pt uptake in the acidic pH range clustered around a final pH of 3 (figure 3(b)), which will be attributed to ion exchange in the discussion. The adsorption/exchange data with 60 ppm (corresponding to 30% exchange) of PTA appears to be pH independent ion exchange, roughly constant over the entire pH range. This agrees with earlier results obtained in our laboratory for low concentration (low exchange per cent)

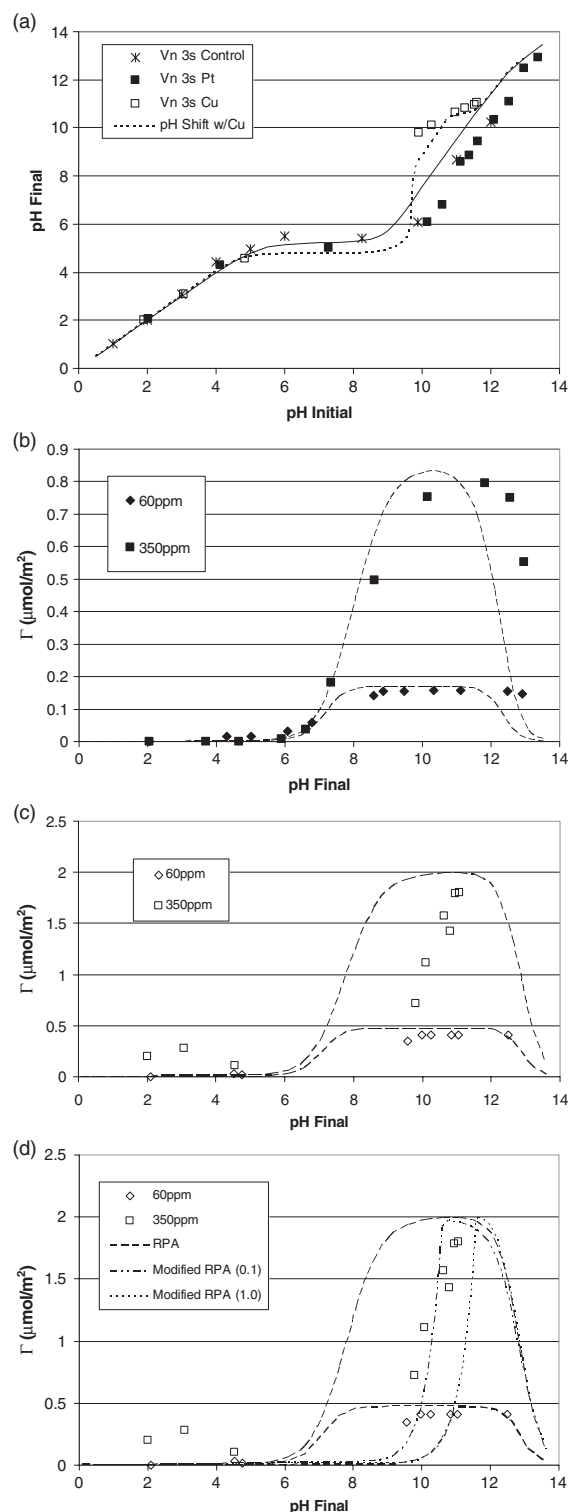


Figure 2. Pt and Cu adsorption onto silica: (a) pH shifts with and without metals; (b) PTA uptake versus final pH; (c) CTA uptake versus final pH; model parameters $\text{PZC} = 4.0$, $\Delta\text{p}K = 7.25$, (d) CTA uptake with modified model (see discussion).

solutions [37]. As the concentration of PTA is increased to 160 ppm (100% exchange), there is a slight increase in PTA exchange in the acidic pH region and an increase in uptake as the pH is increased. The lower, dotted line in figure 3(b) represents 100% exchange, while the upper dashed

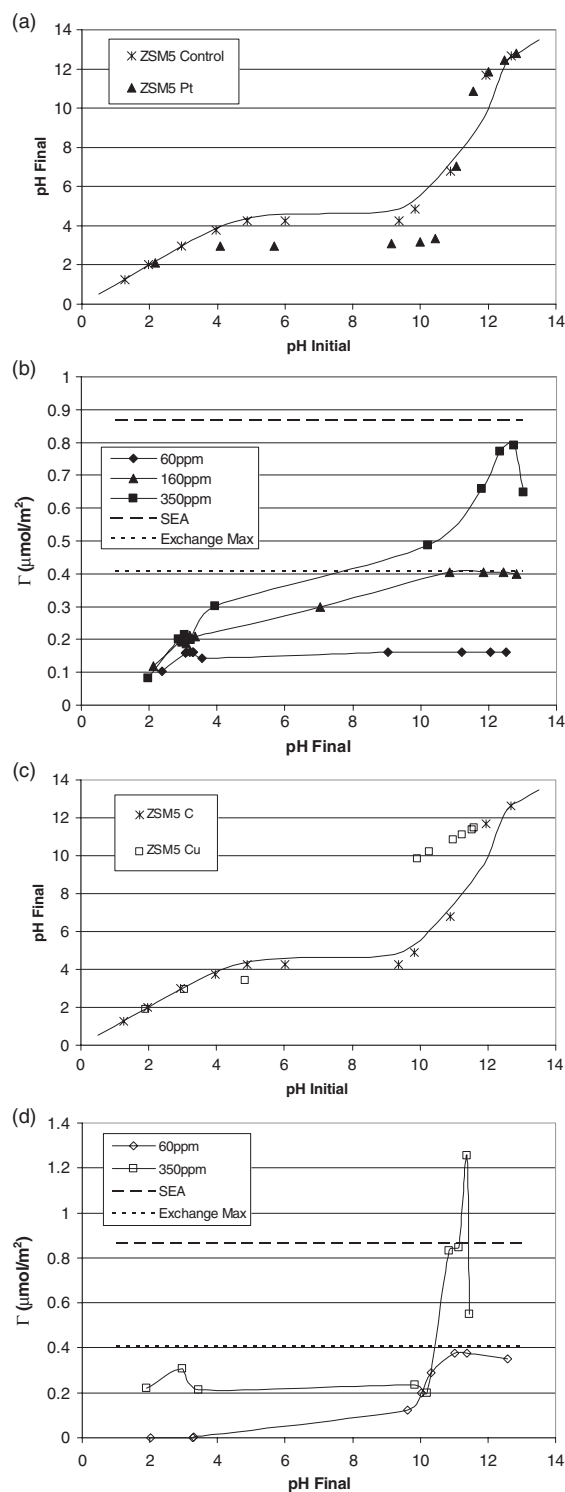


Figure 3. Pt and Cu adsorption onto H-ZSM5: (a) pH shift data with and without Pt; (b) PTA uptake versus final pH; (c) pH shift data with and without Cu; (d) CTA uptake versus final pH; model parameters $PZC = 3.0$, $\Delta pK = 5.0$.

line represents the physical maximum determined from PTA adsorption data on silica ($0.86 \mu\text{mol m}^{-2}$, [17]). Uptake corresponding to full (100%) exchange of the 160 ppm solution is only seen at the highest pH values. With 350 ppm PTA in

solution, the exchange of PTA at the lower pH region was similar to that found with 160 ppm PTA in solution. As the pH was increased, an increase in PTA uptake above 100% exchange was observed, with a maximum of $0.79 \mu\text{mol m}^{-2}$.

The pH shifts for metal free and copper containing solution over H-ZSM5 are shown in figure 3(c). In the lower pH region the deviation of the metal free and metal containing pH shifts are again indicative of ion exchange of the bare metal copper cation with two protons. In the basic pH region, pH shift data containing CTA in solution is well above the pH shift data without metal in solution. This trend is similar to that found on silica and will be discussed later. The adsorption/exchange data of copper onto H-ZSM5 are reported in figure 3(d). At the lower concentration of copper (60 ppm), exchange in the lower acidic region was negligible for both the 1 h and 24 h data. With an increase in pH, CTA adsorption increased and levelled off. With an increase in the concentration of copper, uptake of Cu, presumably as the bare metal ion, was observed, similar to PTA. For both metals the maximum extent of exchange at low pH is about 50%. With an increase in pH, the adsorption of CTA increased to a maximum of $1.25 \mu\text{mol m}^{-2}$, which mirrors the higher surface density of CTA relative to PTA over silica (figure 2).

The pH shift data over Na mordenite with and without platinum in solution are displayed in figure 4(a). The smaller drops in pH with PTA in solution are again due to exchange with protons, but since this zeolite mainly contained Na^+ and not protons the pH shifts are not as large as seen with the ZSM5. The PTA uptake curves at 60, 160 and 400 ppm on Na mordenite are given in figure 4(b). The adsorption/exchange data with 60 ppm (30% exchange) of PTA appear to be pH-independent ion exchange, roughly constant over the entire pH range, similar to the data obtained by Spieker and Regalbuto [37]. As the concentration of PTA is increased to 160 ppm (100% exchange), there is a slight increase in PTA exchange in the acidic pH region. As the pH is increased, there is a maximum in PTA adsorption approaching 100% exchange, with a decrease in uptake at the extreme pH regions, similar to PTA adsorption over silica (figure 2(b) and [17]). With 350 ppm PTA in solution, the adsorption data over the entire pH region appeared to be similar to the adsorption data with 160 ppm PTA in solution.

Figure 4(c) displays the pH shift results for metal free and copper containing solution over Na mordenite. In the lower pH range the decreases in pH of the metal containing solutions are again due to some proton exchange. In the basic pH region, pH shifts for CTA solutions are still above the pH shifts for metal-free solutions but are shifted less than the silica and H-ZSM5 curves (figures 3(a) and (c)). The uptake of copper onto Na mordenite is reported in figure 4(d). At the lower concentration of copper (60 ppm), exchange was fairly constant around $0.5 \mu\text{mol m}^{-2}$ over almost the entire pH range, with decreases at the pH extremes. With an increase in the concentration of copper, a slight increase in exchange of the bare metal ion was observed similar to that observed with PTA. The maximum exchange in the low pH region is again about 50% for both metals. With an increase in pH, the adsorption of CTA increased to a maximum of about $2 \mu\text{mol m}^{-2}$, slightly over 100% exchange, with a decrease at the most basic pH. The adsorption curves of CTA and PTA onto Na mordenite are very similar.

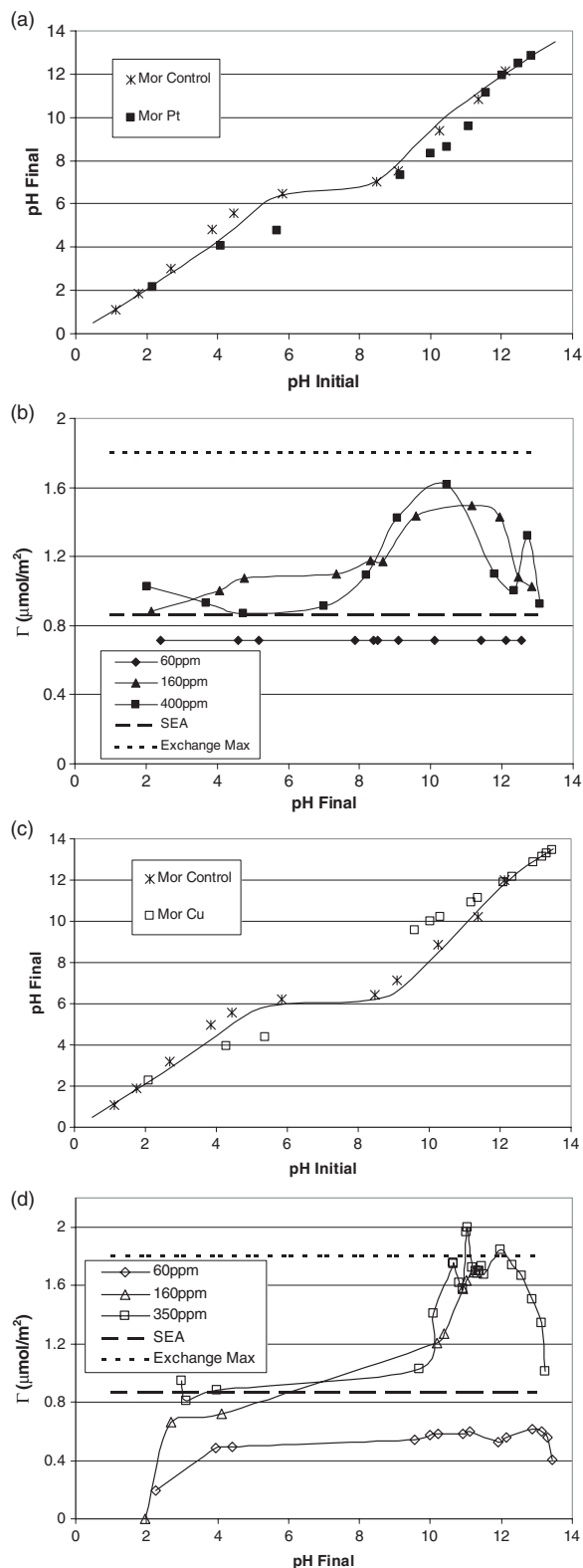


Figure 4. Pt and Cu adsorption onto Na-MOR: (a) pH shift data with and without Pt; (b) PTA uptake versus final pH; (c) pH shift data with and without Cu; (d) CTA uptake versus final pH; model parameters $\text{PZC} = 6.0$, $\Delta\text{p}K = 5.0$.

The pH shift data over Na-Y54 with and without platinum in solution is displayed in figure 5(a). The pH shift data with

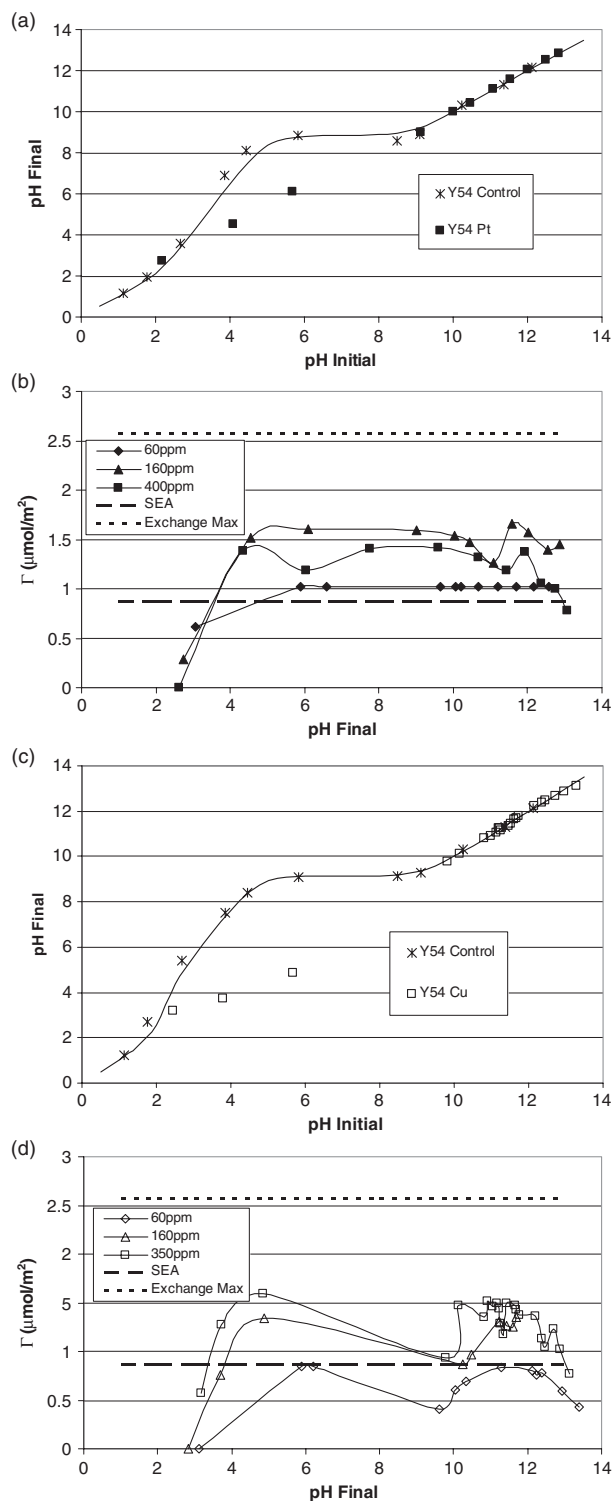


Figure 5. Pt and Cu adsorption onto Na-Y54: (a) pH shift data with and without Pt; (b) PTA uptake versus final pH; (c) pH shift data with and without Cu; (d) CTA uptake versus final pH; model parameters $\text{PZC} = 10.0$, $\Delta\text{p}K = 5.0$.

PTA in solution are again indicative of some proton exchange for PTA in the lower to mid pH range, but not nearly so much as in the case of the fully protonated H-ZSM5 since the Y54 contains mostly Na^+ counter-ions. The PTA uptake curves at 60, 160 and 400 ppm on Na-Y54 are given in figure 5(b).

The adsorption/exchange data with 60 ppm (30% exchange) of PTA appears to be pH independent ion exchange, roughly constant over the entire pH range. The low uptake at the very lowest pH values, in this and other figures, is likely due to the dissolution of Al from the zeolite lattice [38, 39]. Y-54 with high Al content would be the least stable material at low pH. As the concentration of PTA was increased to 160 ppm (100% exchange), there is a modest increase in PTA exchange at most pH values. The surface density is between that of SEA and the exchange maximum. The 350 ppm PTA solution behaves similarly to the 160 ppm solution; in both sets of data there may appear a faint volcano shape at high pH, indicative of SEA, as seen for H-ZSM5 and Na-MOR (figures 3(b) and 4(b)).

Figure 5(c) displays the pH shifts for metal free and copper containing solutions over Na-Y54. A relative decrease of pH in the lower range again indicates some exchange with protons. In the basic pH region, the pH of CTA containing solution is now not shifted up as occurred with silica and H-ZSM5 and to a lesser extent with mordenite, but is in fact similar to the pH shift data without metal in solution. The uptake of copper onto Na-Y54 is reported in figure 5(d). There appear to be two groupings of the data, one at lower and one at higher pH. The bare metal ion in the lower pH regions increased in uptake as the concentration was increased, typical of an exchange reaction. However, 100% exchange was never achieved. Once again the maximum extent of exchange for both metals is around 50%. In the basic pH region, CTA shows a mild pH dependence, a little more pronounced than for PTA.

5. Discussion

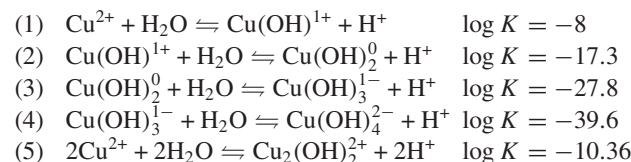
5.1. Pt and Cu adsorption onto silica

In figure 2(a) the virtual overlap of the pH shifts for the Pt solutions with the metal free control experiment, as well as reasonable agreement of the RPA model to the data, indicate that adsorption of Pt amines over silica is electrostatic in nature. Pt adsorption and the proton chemistry of the surface hydroxyl groups are independent; that is, the silica surface deprotonates regardless of whether Pt is in solution; in the presence of a negatively charged silica surface Pt cations will adsorb. The most direct characterization of the nature of adsorbed Pt ammine complexes has recently been accomplished using x-ray reflectivity methods; these confirmed that Pt amines adsorb as outer sphere complexes over hydroxyl-terminated quartz surfaces [40]. We have argued previously [17] that ‘strong electrostatic adsorption’ is a much more accurate description of Pt uptake onto silica than the oft-cited mechanism of ‘ion exchange’ [41, 42].

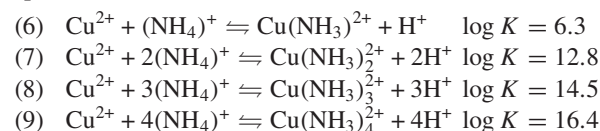
At low to mid pH, there is little Cu uptake and no downward pH shift in figure 2(a) that would indicate the exchange of Cu (bare metal) ions for protons from the surface hydroxyl groups. The behaviour of Cu amines at high pH is more complex than Pt, as immediately noted in the upward pH shifts relative to the control experiment; upon adsorption, hydroxyls are generated. This upward shift in pH is responsible for the large discrepancy of the RPA model in figure 2(c).

The explanation for this difference may lie in the weaker stability of the Cu tetra-ammine complex relative to the Pt tetra-ammine complex. The hydrolysis of copper has been well

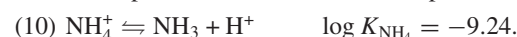
documented by Baes and Messmer [43] and follows reactions (1)–(5).



With the addition of NH_4OH the copper forms the ammine species and follows reactions (6)–(9).



With the deprotonation of the ammonia species as



Figures 6(a)–(c) display the speciation of copper (a) without addition of ammonia, (b) with the addition of ammonia to raise the pH and with the addition of ammonia to raise the pH in addition to 0.2 M NH_4NO_3 as the background electrolyte.

Louis and co-workers [21] determined that with the background electrolyte (NH_4NO_3) it was the tetra-ammine that was attracted to the negatively charged surface, supporting the speciation of copper in figure 6(c). In following studies [22, 23], Louis and co-workers did not use a background electrolyte in solution. They reported similar pH shifts observed in this study. They determined that over an increased period of time, a copper phyllosilicate forms on the surface.

In the present study, short contact times were employed, similar to those used to make overexchanged copper/ZSM5 catalysts [4]. No background ammonia was used, so conditions most closely correspond to figure 6(b), where the hydroxyl-bridged $\text{Cu}_2(\text{OH})_2^{2+}$ dimer dominates in the pH range from 6.5 to 10.5. In figure 2(c), the uptake of Cu occurs between 10 and 11.5. According to figure 6(b), the dominant species in the bulk of the solution should be tetra-ammines. However, as the Cu complex approaches the surface there is a decrease in the local pH, according to electric double-layer theory [17, 31–33, 36]. The change in pH approaching the adsorption plane is shown in figure 7, for the silica surface with a PZC of 4, and the other zeolites. The pH at the adsorption plane of silica, for a bulk pH of 11.0, is predicted to be 7.3. We postulate that the copper tetra-ammine is physically attracted to the negatively charged silica surface. As it approaches the surface, the pH near the surface becomes more acidic, and following figure 6(b) the copper dimer forms. Formation of the dimer releases ammonia ligands, some of which will convert to ammonium ions (though not many since the pH is above $\text{p}K_{\text{NH}_4} = 9.2$), and consequently raise the pH.

This release of ammonia and conversion to ammonium cannot be quantified but can be used as justification to modify the RPA model. Figure 2 shows the simulated pH shifts (figure 2(a)) and Cu uptake curves (figure 2(d)) in which the final pH has been adjusted by assuming a ratio of ammonia converted to ammonium per ammonia released. A ratio of 1 shifts the pH values too far to the right; a ratio of 0.1 best fits both the adsorption data and the pH shift data. This ratio is consistent with the low conversion of ammonia to

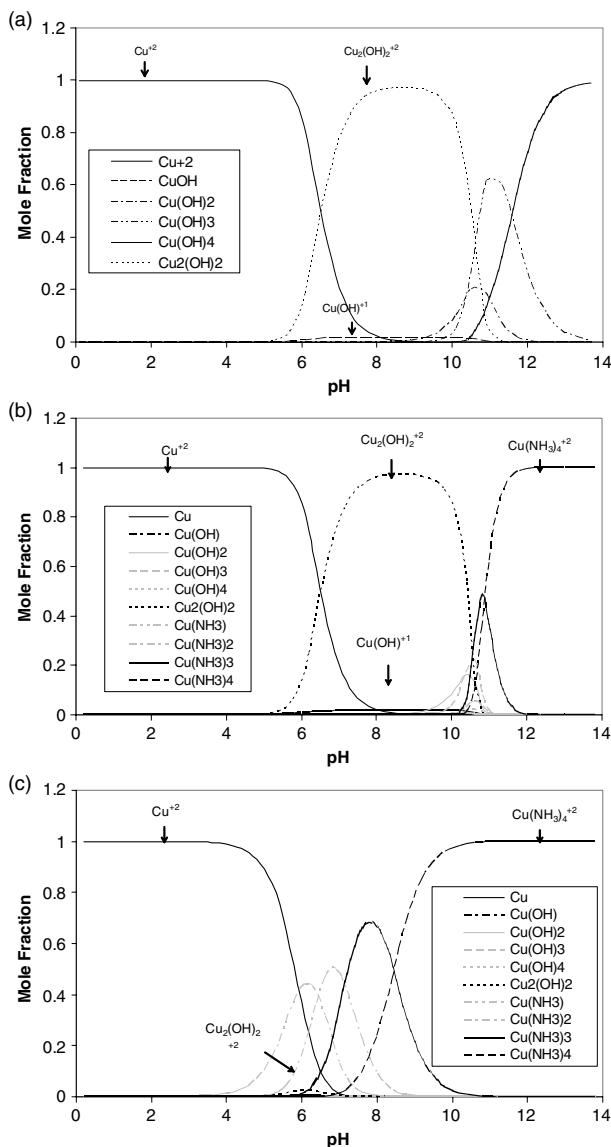


Figure 6. Copper hydrolysis with (a) no ammonia, (b) ammonia addition to increase pH, and (c) ammonia addition with 0.2 M NH_4NO_3 as a background electrolyte.

ammonium at pH higher than pK_{NH_4} . Realistically, this ratio would change with pH, and could in principle be used to obtain an even better fit, but that detail is not warranted for our purpose. We only wish to suggest that the pH shifts seen here, and the existence of the hydroxyl-bridged Cu dimer observed by others [9, 8], could well be due to a response of the adsorbing CTA complex to changes in the local pH. This explanation has been used to explain the change in speciation of Pt oxychloride complexes [44] and gold oxychloride complexes [45] adsorbing over alumina. The Pt tetra-ammine complex is more stable and so does not give rise to these shifts.

As a final note, respeciation to the copper dimer also explains the higher adsorption density of Cu relative to Pt. The size of the Cu ammine complex, at 2.55 Å, is similar to that of PTA (2.41 Å). The more than twofold higher surface density of Cu is then consistent with the formation and electrostatic deposition of the cationic $[\text{Cu}_2(\text{OH})_2]^{2+}$ complex.

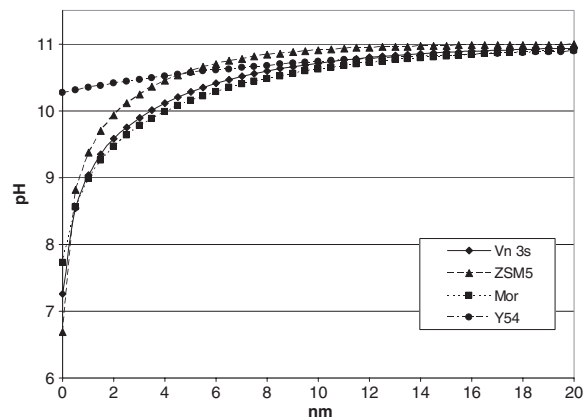


Figure 7. pH as a function of approach to the surface of silica, HZSM5, Na-MOR and Na-Y54at bulk pH 11.

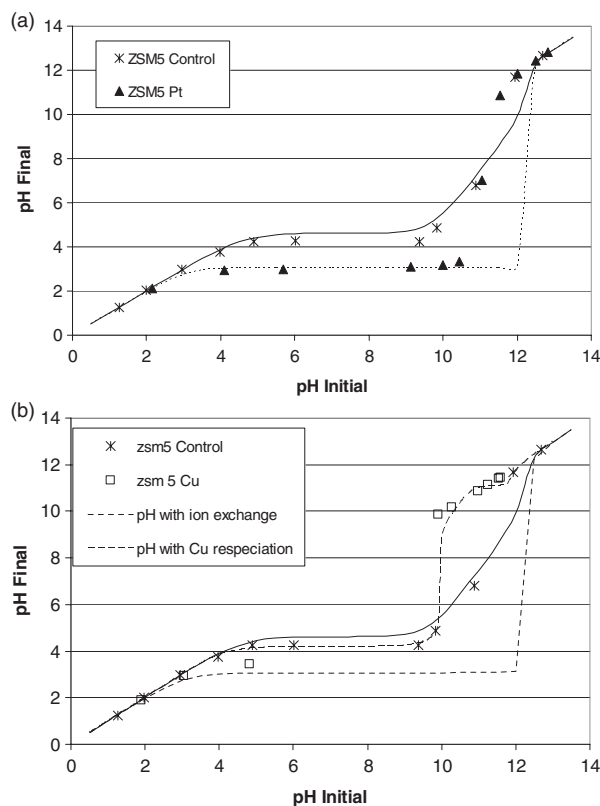
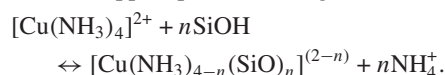


Figure 8. Simulation of pH shifts of ZSM5 for (a) Pt and (b) Cu adsorption; experimental data taken from figures 3(a) and (c), respectively.

Louis and co-workers demonstrated the electrostatic nature of copper adsorption onto silica [21–23]. In their comprehensive study, the copper tetra-ammine was adsorbed onto silica at a high pH with a background electrolyte of NH_4NO_3 . The copper speciation in that case most closely resembles figure 6(c), where CTA is most dominant. With EPR and EXAFS, $\text{Cu}(\text{NH}_3)_4$ was determined to be the adsorbed species, contrary to previous studies by Tominaga *et al* [46, 47] that the copper species exchanged on the silica surface by



Although such an exchange reaction would explain the increase in pH shift of the CTA adsorption data observed in this study, in the basic region, the majority of the surface species would be deprotonated and negatively charged. Such a reaction would be improbable. We believe the mechanism most consistent with the solution conditions employed here is electrostatic adsorption of Cu ammine followed by respeciation to the Cu dimer at the local pH of the adsorption plane.

5.2. Pt and Cu uptake by zeolites

If it is assumed that electrostatic adsorption occurs in the same high pH range where it occurs over silica, we can attribute uptake in the mid to low range as ion exchange. If such is the case, full exchange was not achieved for either metal over any of the three zeolites. The maximum exchange observed in the acidic to neutral pH region for these three zeolites were for Pt 44% (ZSM5), 57% (mordenite) and 62% (Y54), and for Cu 51% (ZSM5), 49% (mordenite) and 62% (Y54) in figures 3, 4, and 5 respectively. There could be two reasons for this; first, ion exchange of Pt and Cu is limited to the supercages and large channels, while aluminium is substituted throughout the zeolite structure [48–52]. The diameter of the PTA complex is 4.82 Å, which should fit only into the larger channels of each zeolite (5.5 by 5.1 Å and 5.3 by 5.6 Å for MFI, 7.0 by 6.5 Å for mordenites and 7.4 Å for faujasites [48–52]) provided it loses its hydration sheaths. On the other hand, the exchange of smaller Cu^{2+} ions (1.45 Å diameter), which exist up to a pH of about 6 (figure 6), was very similar to that of the Pt tetra-ammine. The smaller adsorbate might be expected to in all pores and show a higher degree of exchange. The second explanation is that, since two aluminium sites are necessary for one PTA molecule to exchange, large distances between Al sites may also prohibit 100% exchange. The aluminium weight per cent for ZSM5, mordenite and Y54 used in this study was 1.0, 3.87 and 8.91%. The exchange trends of both metals reflect the aluminium content, if only mildly. The similarity of the exchange percentages of the two differently sized adsorbates supports the second explanation.

The delineation of ion exchange and electrostatic adsorption can be made by a closer inspection of the pH shift data over the HZSM5 sample in figures 2 and 3. These data have been reproduced in figure 8 for each metal with an additional model curve calculated by assuming that two protons exchange for each Pt or Cu adsorbed. In figure 8(a), for PTA, the ‘ion exchange’ pH shift agrees with the data in the low and mid pH range. At high pH, however, the ion exchange calculation predicts low pH through initial pH values of 12. Above 10.5, where the majority of Pt is adsorbed (figure 3(b)), the final pH is not low as predicted by ion exchange but overlaps with the control experiment, as occurred during adsorption over silica (figure 2). This result suggests that the mechanism of interaction shifts between ion exchange and electrostatic adsorption at a pH of about 10–11. This range agrees with the values employed by Chester *et al* [18] and Smirnov [20], where overexchange of Pt was reported. The characteristic high pH volcano shape as well as maximum surface density (near $0.8 \mu\text{mol m}^{-2}$) of electrostatic adsorption is also seen (figure 3(b)). Thus we attribute ‘overexchange’ of Pt amines not to ‘ion exchange’ over silanol groups [18, 20], but to SEA over deprotonated silanol groups, as over silica [17].

The situation with copper is similar, but with added complexity that can be explained by the respeciation of the Cu ammine complex adsorbing at high pH. The pH shifts for the Cu/ZSM5 system are shown again in figure 8(b) with two additional model curves. The first, predicted for ion exchange, assumes two protons/Cu and falls a bit below what is unfortunately the only the experimental point in this range. Ion exchange clearly does not account for the upward pH shifts in the high pH range; protons are consumed and not generated.

To explain this consumption of protons, the same argument as used earlier for silica can be employed. The PZC of the HZSM5 is 3, a little lower than silica. The pH at the adsorption plane of ZSM5 for a bulk pH of 11, shown in figure 7, is 6.7, close to that of silica. Thus the same lowering of local pH upon adsorption, caused by respeciation of Cu ammine to the $\text{Cu}_2(\text{OH})_2^{2+}$ dimer, the release of ammine ligands and their partial conversion to ammonium, should occur over ZSM5 as it does over silica. The upward pH shift over ZSM5 in the high pH range (figures 3(c) and 8(b)) is very similar to that over silica (figure 2(a)). The pH shifts are more accurately modelled with respeciation at high pH, which is shown in the third model curve of figure 8(b). The higher surface density of Cu compared to Pt over silica at high pH is also mirrored in the high pH uptake over ZSM5 (figures 3(b) and (d)). Both pH shifts and uptake density again are consistent with the conversion to the hydroxyl-bridged dimer.

Sachtler and co-workers presented much evidence that Cu–O–Cu dimers are present in reduced, overexchanged Cu/ZSM5 catalysts, and also suggest that the adsorbed precursor is the hydroxyl-bridged dimer $[\text{Cu}_2(\text{OH})_2]^{2+}$ [14]. (Since the dimer is EPR silent, Louis and co-workers would not have observed such a species present on silica [21–23].) We propose that the pathway to the formation of this dimer on ZSM5, as on silica, is through electrostatic adsorption of amines at high pH followed by respeciation at the local pH.

In the progression from HZSM5 to Na-MOR to NaY54, the aluminium content and the PZC go up. These trends explain the adsorption and pH shift results seen in figures 4 and 5. The characteristic volcano shape of electrostatic adsorption is clearly evident and similar for both metals over the Na mordenite (figure 4), but is smaller in proportion to the amount of ion exchange. Only traces of electrostatic adsorption appear for either metal in the uptake data over Na Y54 (figure 5). This is expected, per figure 1, when the aluminium content increases and the exchange capacity dominates electrostatic adsorption. The density of metal ions exchanged increases from about $0.2 \mu\text{mol m}^{-2}$ for the low aluminium ZSM5 to $0.8 \mu\text{mol m}^{-2}$ for mordenite to about $1.5 \mu\text{mol m}^{-2}$ for the high aluminium faujasite.

The trend in the pH shifts also follows this progression. There is less downward shift in pH for each metal from ion exchange due to the fact that the counterions in the mordenite and faujasite are mainly Na^+ and not H^+ . In the high pH range Cu adsorption data over mordenite (figure 4(c)), there are again upward shifts in the pH, but these are not as pronounced as in the case of silica and HZSM5. Over Y54 (figure 5(c)) there are no upward shifts. The explanation is given in figure 7, where the pH at the adsorption plane of these two materials, which have PZCs of 6 and 10, is seen to be 7.7 and 10.3, respectively. A smaller degree of respeciation would

be expected over mordenite, while over Y54 the Cu species should remain entirely as an ammine (figure 6(b)).

6. Conclusions

It appears that metal amines interact with zeolites by a dual mechanism involving both ion exchange and electrostatic adsorption, the former being the dominant mechanism in the low to mid pH range, and the latter operating at high pH. This effect is most clearly manifested in zeolites with low aluminium content such as ZSM5. Differences between Pt and Cu amines can be explained by the weaker stability of the Cu tetra-ammine complex and the change in local pH near the surface of low PZC zeolites, which is a feature of electrostatic adsorption. As the local pH lowers, the copper tetra-ammine, $[(\text{NH}_3)_4\text{Cu}]^{2+}$ is converted to the hydroxylated copper dimer, $\text{Cu}_2(\text{OH})_2^{2+}$. A portion of the released ammonia converts to ammonium ions, consuming protons and increasing the solution pH. In high PZC, high aluminium zeolites, ion exchange dominates almost completely and there is no conversion of CTA to the dimer.

References

- [1] Iwamoto M *et al* 1989 *Chem. Lett.* 213–6
- [2] Iwamoto M *et al* 1990 *Chem. Lett.* 1967–70
- [3] Ganemi B, Bjornbom E, Demirel B and Paul J 2000 *Microporous Mesoporous Mater.* **38** 287–300
- [4] Ohman L O *et al* 2002 *Mater. Chem. Phys.* **73** 263–7
- [5] Soria J *et al* 2000 *J. Catal.* **190** 352–63
- [6] Gervasini A, Picciau C and Auroux A 2000 *Microporous Mesoporous Mater.* **35** 457–69
- [7] Sato S, Yu-u Y, Yahiro H, Mizuno N and Iwamoto M 1991 *Appl. Catal.* **70** L1–5
- [8] Iwamoto M and Hamada H 1991 *Catal. Today* **10** 57–71
- [9] Yahiro H and Iwamoto M 2001 *Appl. Catal. A* **222** 163–81
- [10] Curtin T, Grange P and Delmon B 1997 *Catal. Today* **36** 57–64
- [11] Millar G J *et al* 1999 *J. Catal.* **183** 161–81
- [12] Parvulescu V I, Centeno M A, Grange P and Delmon B 2000 *J. Catal.* **191** 445–55
- [13] Lei G D, Adelman B J, Sarkany J and Sachtler W M H 1995 *Appl. Catal. B* **5** 245–56
- [14] Yan J Y, Sachtler W M H and Kung H H 1997 *Catal. Today* **33** 279–90
- [15] Shin H K *et al* 1995 *Catal. Today* **26** 13–21
- [16] Guo J *et al* 1995 *JSAE Rev.* **16** 21–5
- [17] Schreier M and Regalbuto J R 2004 *J. Catal.* **225** 190–202
- [18] Chester A W *et al* 1985 *J. Chem. Soc., Chem. Commun.* 289–90
- [19] Woolery G L, Alemany L B, Dessau R M and Chester A W 1986 *Zeolites* **6** 14–6
- [20] Smirnov A V *et al* 2000 *J. Catal.* **194** 266–77
- [21] Trouillet L, Toupance T, Villain F and Louis C 2000 *Phys. Chem. Chem. Phys.* **2** 2005–14
- [22] Toupance T, Kermarec M and Louis C 2000 *J. Phys. Chem. B* **104** 965–72
- [23] Toupance T, Kermarec M, Lambert J F and Louis C 2002 *J. Phys. Chem. B* **106** 2277–86
- [24] Arrua L A *et al* 1997 *Appl. Catal. A* **165** 259–71
- [25] Arrua L A *et al* 2000 *Appl. Catal. A* **204** 33–48
- [26] Shimokawabe M, Takezawa N and Kobayashi H 1982 *Appl. Catal.* **2** 379–87
- [27] Torre-Abreu C, Ribeiro M F, Henriques C and Delahay G 1997 *Appl. Catal. B* **14** 261–72
- [28] Shimokawabe M, Takodoro K, Sasaki S and Takezawa N 1998 *Appl. Catal. A* **166** 215–23
- [29] Shimokawabe M, Hirano K and Takezawa N 1998 *Catal. Today* **45** 117–22
- [30] Cheung T, Bhargava S K, Hobday M and Fogar K 1996 *J. Catal.* **158** 301–10
- [31] Agashe K A and Regalbuto J R 1997 *J. Colloid Interface Sci.* **185** 174
- [32] Spieker W A and Regalbuto J R 2001 *Chem. Eng. Sci.* **56** 3491–504
- [33] Hao X and Regalbuto J R 2003 *J. Colloid Interface Sci.* **267** 259
- [34] Brunelle J P 1978 *Pure Appl. Chem.* **50** 1211
- [35] Santhanam N, Conforti T A, Spieker W and Regalbuto J R 1994 *Catal. Today* **21** 141–56
- [36] Park J and Regalbuto J R 1995 *J. Colloid Interface Sci.* **175** 239
- [37] Regalbuto J R and Antos G J 2004 *Naphtha Reforming* ed G J Antos (New York: Dekker) chapter 5 (Preparation of Reforming Catalysts)
- [38] McDaniel C V and Maher P K 1976 *Zeolite Chemistry and Catalysis (ACS Monograph vol 171)* ed J A Rabo (Washington, DC: American Chemical Society) chapter 4, pp 285–331
- [39] Dyer A 1988 *An Introduction to Zeolite Molecular Sieves* (New York: Wiley)
- [40] Park C, Fenter P, Sturchio N and Regalbuto J R 2005 *Phys. Rev. Lett.* **94** 076104
- [41] Benesi H A, Curtis R M and Studer H P 1968 *J. Catal.* **10** 328
- [42] Goguet A *et al* 2002 *J. Catal.* **209** 135
- [43] Baes C F Jr and Messmer R E 1986 *Hydrolysis of Cations* (Malabar, FL: Krieger) (ISBN: 0898748925)
- [44] Spieker W, Liu J, Hao X, Miller J T, Kropf J and Regalbuto J R 2003 *Appl. Catal. A* **243** 53
- [45] Yang J Y *et al* 2005 *Appl. Catal. A* at press
- [46] Tominaga H, Ono Y and Keei T 1975 *J. Catal.* **40** 197
- [47] Tominaga H, Kaneko M and Ono Y 1977 *J. Catal.* **50** 400
- [48] Olson D H, Kokotailo G T, Lawton S L and Meier W M 1981 *J. Phys. Chem.* **85** 2238–43
- [49] Kokotailo G T, Lawton S L, Olson D H and Meier W M 1978 *Nature* **272** 437–8
- [50] Bergerhoff G, Baur W H and Nowacki W N 1958 *Jahrb. Miner. Mh.* 193–200
- [51] Baur W H 1964 *Am. Mineral.* **49** 697–704
- [52] Meier W M 1961 *Z. Kristallogr.* **115** 439–50